Substantial Nuclear Hyperfine Mixing Effect in Boronlike ^{205}Pb Ions

Wu Wang[1,2] and Xu Wang[1,3,*]

[1]Graduate School, China Academy of Engineering Physics, Beijing 100193, China
[2]Center for Theoretical Physics and School of Physics and Optoelectronic Engineering, Hainan University, Haikou, Hainan 570228, China
[3]Southern Center for Nuclear-Science Theory, Institute of Modern Physics, Chinese Academy of Sciences, Huizhou, Guangdong 516000, China

(Received 8 October 2023; revised 26 December 2023; accepted 7 June 2024; published 16 July 2024)

Nuclear hyperfine mixing (NHM) is a distinctive effect through which nuclear properties and dynamics can be efficiently controlled. Traditionally, the scientific consensus has predominantly associated NHM with its pronounced impact on ^{229}Th, owing to the existence of its low-lying isomeric state. However, in the present study, by developing a general theory for NHM, we predict a surprisingly substantial NHM effect in boronlike ^{205}Pb ions (specifically, $^{205}Pb^{77+}$), featuring a nuclear transition energy of 2.329 keV. The radiative lifetime of the ^{205}Pb isomer is reduced by 4 orders of magnitude, from 15 min to 32 ms. This remarkable and unexpected NHM effect stems from a heretofore unexplored process: an opening of a magnetic dipole channel that is otherwise forbidden without NHM. ^{205}Pb ions now emerge as an attractive alternative candidate for experimental validation and investigation of the NHM effect.

DOI: 10.1103/PhysRevLett.133.032501

Introduction.—Nuclear isomers, characterized by their relatively extended lifetimes, typically exceeding 1 ns, play important roles in both fundamental nuclear physics [1] and nuclear astrophysics [2,3]. Beyond their fundamental significance, nuclear isomers exhibit intriguing potential applications in nuclear optical clocks [4–7], nuclear energy storage [8–10], nuclear lasers [11–13], etc. Active control of nuclear isomers is the basis of realizing these applications. Various methods have been attempted or proposed, involving the use of electrons [14–18], x rays [19–22], and intense laser pulses [23–27], among others. These methods predominantly focus on exciting the isomers without altering their inherent properties, such as the radiative lifetime—a pivotal parameter for these applications.

In this context, nuclear hyperfine mixing (NHM), also known as nuclear spin mixing in hyperfine fields [28,29], emerges as a unique phenomenon capable of modulating the radiative lifetime of nuclear isomers. This effect arises when an unpaired bound electron generates a potent electromagnetic field near the nucleus, leading to the mixing of different nuclear states through hyperfine (or more general electromagnetic) interactions. It has been a prevailing belief that NHM predominantly influences highly charged ^{229}Th ions due to the existence of a low-lying isomeric state just 8 eV above the nuclear ground state, facilitating efficient mixing due to the minuscule nuclear transition energy [29,30]. Indeed, the NHM effect exerts significant influence on hydrogenlike ^{229}Th ions (i.e., the $^{229}Th^{89+}$ ion), causing a remarkable reduction of the isomer's radiative lifetime by 5 orders of magnitude [31]. Consequently, studies on the NHM effect have been dominantly restricted to highly charged ^{229}Th ions during the past three decades [29–36]. However, experimental verification of the NHM effect has been hindered by the complexities of obtaining ^{229}Th and detecting its radiative decay signal [37–40].

In this Letter, we identify another nuclear isomer, specifically ^{205}Pb, also exhibiting a substantial NHM effect. This isomer holds significant astrophysical relevance as previously indicated [41–43]. We unveil a 4-orders-of-magnitude reduction in the radiative life time of the isomer from 15 min in the bare nucleus state ($^{205}Pb^{82+}$) to mere 32 ms in its boronlike (B-like) ionic state ($^{205}Pb^{77+}$). What is surprising and unexpected is that this isomer has an excitation energy of 2.329 keV [44], conventionally considered to be too large for efficient NHM. Given its accessibility and cost-effectiveness, the ^{205}Pb ion emerges as a promising alternative for experimental validation and investigation of the NHM effect. This revelation opens new avenues for exploring and harnessing NHM across a broader spectrum of nuclear isomers, enhancing the field's potential applications.

We find that this remarkable NHM effect arises from a hitherto unexplored mechanism: the involvement of an electronic excited state in the NHM process. This participation leads to the opening of a more efficient magnetic dipole ($M1$) transition channel amid the existing electric quadrupole ($E2$) channels. Consequently, not only does the radiative lifetime alter, but also the angular momentum of the emitted photons changes.

General theory of NHM.—The nucleus-electron system can be described by the Hamiltonian

$$H = H_e + H_n + H_{\rm en}, \tag{1}$$

where H_e and H_n are the Hamiltonian of the atomic electrons and of the nucleus, respectively. $H_{\rm en}$ is the electron-nucleus electromagnetic interaction, and it can be written as a summation over irreducible tensor operators [45]:

$$H_{\rm en} = \sum_{\tau=E,M}\sum_{Lm}(-1)^m \mathcal{M}^{\tau}_{L-m} T^{\tau}_{Lm}, \tag{2}$$

where $\mathcal{M}^{\tau}_{Lm}$ and T^{τ}_{Lm} are the multipole operators of rank L for the atomic nucleus and for the electrons, respectively. The explicit expressions of $\mathcal{M}^{\tau}_{Lm}$ and T^{τ}_{Lm} can be found in the literature, e.g., Refs. [27,45], respectively. Here, $\tau = E$ or M denotes electric or magnetic multipoles.

In the absence of the interaction $H_{\rm en}$, the system is described by the product of nuclear state $|Im_I\rangle$ with nuclear spin I and electronic state $|\gamma J m_J\rangle$ with angular momentum J, where m_I and m_J are nuclear and electronic magnetic quantum numbers, respectively, and γ contains all other electronic quantum numbers. With the interaction, the nuclear spin I and the electronic angular momentum J are coupled to form a total angular momentum F. The coupled basis can be written as

$$|Fm_F(I\gamma J)\rangle = \sum_{m_I m_J} C(F,I,J;m_F,m_I,m_J)|Im_I\rangle|\gamma J m_J\rangle, \tag{3}$$

where m_F is the projection of the total angular momentum F and $C(F,I,J;m_F,m_I,m_J)$ is a Clebsch-Gordan coefficient. For the electron(s) in the ground state $|\gamma_\varepsilon J_\varepsilon m_{J_\varepsilon}\rangle$, the nuclear hyperfine levels are obtained: $|F_\mu m_{F_\mu}\rangle \equiv |Fm_F(I_\mu\gamma_\varepsilon J_\varepsilon)\rangle$. Here, we use μ (ε) to denote the nuclear state (electronic state).

NHM can be described using perturbation theory as

$$|F_\mu m_{F_\mu}\rangle_+ = |F_\mu m_{F_\mu}\rangle + \sum_{\mu'\varepsilon'} c_{\mu\varepsilon,\mu'\varepsilon'}|Fm_F(I_{\mu'}\gamma_{\varepsilon'}J_{\varepsilon'})\rangle, \tag{4}$$

where the ket with a plus-sign subscript denotes a state with NHM included and $c_{\mu\varepsilon,\mu'\varepsilon'}$ is a mixing coefficient:

$$c_{\mu\varepsilon,\mu'\varepsilon'} = \frac{(-1)^{I_\mu+J_{\varepsilon'}+F}}{E_{\mu\varepsilon}-E_{\mu'\varepsilon'}}\sum_{L\tau}\begin{Bmatrix} I_{\mu'} & J_{\varepsilon'} & F \\ J_\varepsilon & I_\mu & L\end{Bmatrix} \times \langle I_{\mu'}||M^{\tau}_L||I_\mu\rangle\langle\gamma_{\varepsilon'}J_{\varepsilon'}||T^{\tau}_L||\gamma_\varepsilon J_\varepsilon\rangle. \tag{5}$$

Here, $E_{\mu\varepsilon}$ is the energy corresponding to the state $|Fm_F(I_\mu\gamma_\varepsilon J_\varepsilon)\rangle$. $\langle I_{\mu'}||M^{\tau}_L||I_\mu\rangle$ and $\langle\gamma_{\varepsilon'}J_{\varepsilon'}||T^{\tau}_L||\gamma_\varepsilon J_\varepsilon\rangle$ are the reduced transition matrix elements of the nucleus and of the electrons, respectively. The summation in Eq. (4) contains different nuclear states, leading to the NHM effect. This summation can often be restricted to the nuclear ground state and the isomeric state, if higher states are energetically well separated. For example, for the ^{229}Th nucleus, the energy of the isomeric state is 8.3 eV, while the energy of the second excited state is 29 keV. For the ^{205}Pb nucleus under consideration, the energy of the isomeric state is 2.329 keV, whereas the energy of the second excited state lies at 262.8 keV [44].

With the NHM effect taken into account, the nuclear transition rate (of type order τL) between the isomeric state $|F_e m_{F_e}\rangle_+$ and the ground state $|F_g m_{F_g}\rangle_+$ is calculated as

$$\Gamma = \frac{2K^{[L]}}{[L]!!^2}\frac{L+1}{L}[L] \times \sum_m |{}_+\langle F_g m_{F_g}|t^{\tau}_{Lm} + \mathcal{M}^{\tau}_{Lm}|F_e m_{F_e}\rangle_+|^2, \tag{6}$$

where K is the wave number defined by the nuclear transition energy, the notation $[L]$ represents $2L+1$, and t^{τ}_{Lm} is the multipole transition operator of the electron:

$$t^{E}_{Lm} = \frac{1}{Kc(L+1)}\sqrt{\frac{4\pi}{[L]}}\int \boldsymbol{j}_e\cdot\nabla\times\boldsymbol{L}[r^L Y_{Lm}(\theta,\phi)]\mathrm{d}^3 r,$$
$$t^{M}_{Lm} = \frac{-i}{c(L+1)}\sqrt{\frac{4\pi}{[L]}}\int \boldsymbol{j}_e\cdot\boldsymbol{L}[Y_{Lm}(\theta,\phi)]r^L\mathrm{d}^3 r. \tag{7}$$

Here, $Y_{Lm}(\theta,\phi)$ is spherical harmonics, $\boldsymbol{L} = -i\boldsymbol{r}\times\boldsymbol{\nabla}$ is the angular momentum operator, and $\boldsymbol{j}_e(\boldsymbol{r})$ is the current density operator of the electron.

Averaging over initial states, summing over final states, and using the Wigner-Eckart theorem, the transition rate can be deduced into the following form:

$$\Gamma = \frac{2[L][F_g]K^{[L]}}{[L]!!^2}\frac{L+1}{L}|{}_+\langle F_g||t^{\tau}_L + \mathcal{M}^{\tau}_L||F_e\rangle_+|^2, \tag{8}$$

where ${}_+\langle F_f||\mathcal{M}^{\tau}_L||F_i\rangle_+$ and ${}_+\langle F_f||t^{\tau}_L||F_i\rangle_+$ are reduced transition matrix elements for the nuclear multipole operators $\mathcal{M}^{\tau}_{Lm}$ and the electronic multipole operators t^{τ}_{Lm}, respectively. These matrix elements can be explicitly expressed by utilizing the expansion given in Eq. (4) corresponding to the states $|F_g m_{F_g}\rangle_+$ and $|F_e m_{F_e}\rangle_+$:

$${}_+\langle F_g||\mathcal{M}^{\tau}_L||F_e\rangle_+ = \begin{Bmatrix} I_g & I_e & L \\ F_e & F_g & J_\varepsilon\end{Bmatrix}\langle I_g||\mathcal{M}^{\tau}_L||I_e\rangle, \tag{9}$$

$${}_+\langle F_g||t^{\tau}_L||F_e\rangle_+ = \sum_{\varepsilon'}\Bigg[c_{e\varepsilon,g\varepsilon'}\begin{Bmatrix} J_\varepsilon & J_{\varepsilon'} & L \\ F_e & F_g & I_g\end{Bmatrix}\langle\gamma_\varepsilon J_\varepsilon||t^{\tau}_L||\gamma_{\varepsilon'}J_{\varepsilon'}\rangle + c^*_{g\varepsilon,e\varepsilon'}\begin{Bmatrix} J_{\varepsilon'} & J_\varepsilon & L \\ F_e & F_g & I_e\end{Bmatrix}\langle\gamma_{\varepsilon'}J_{\varepsilon'}||t^{\tau}_L||\gamma_\varepsilon J_\varepsilon\rangle \times(-1)^{J_{\varepsilon'}-J_\varepsilon+I_e-I_g}\Bigg]. \tag{10}$$

Only leading-order terms have been kept. The first matrix element ${}_+\langle F_g||\mathcal{M}^{\tau}_L||F_e\rangle_+$ describes the contribution from

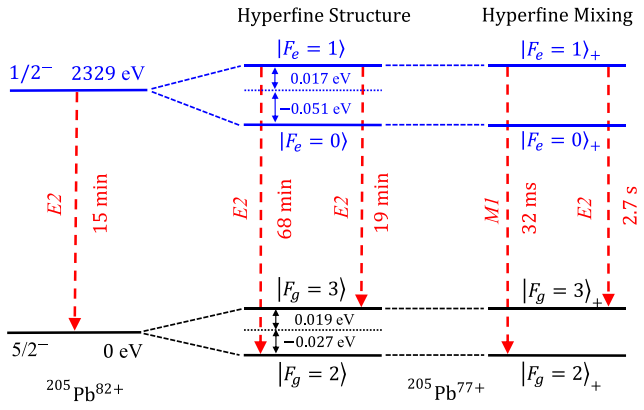

FIG. 1. Left: the ground state and the isomeric state of the bare ^{205}Pb nucleus ($^{205}Pb^{82+}$). Middle: hyperfine structure in the $^{205}Pb^{77+}$ ion without hyperfine mixing. Right: hyperfine mixing in the $^{205}Pb^{77+}$ ion. The additional energy-level shifts caused by hyperfine mixing (on top of the hyperfine structure) are negligibly small, but the transitions are dramatically altered. The most notable change is that the transition between $F_e = 1$ and $F_g = 2$ is now dominated by a newly opened $M1$ transition, which has a much higher rate than the $E2$ counterpart. See Table I for the rates and lifetimes.

the bare nucleus to the transition. The second matrix element ${}_+\langle F_g||t_L^\tau||F_e\rangle_+$, which contains the mixing coefficients given in Eq. (5), describes the transition induced by the NHM effect. It is to be emphasized that Eq. (8) is a general expression for NHM, with all mixing coefficients corresponding to different electronic states and different types of nuclear transition included. In contrast, existing works on the NHM effect [29–36] consider only the mixing coefficients corresponding to the electronic ground state.

Results for ^{205}Pb.—For the ^{205}Pb nucleus, the ground state has spin parity $5/2^-$, and the isomeric state has spin parity $1/2^-$ with energy 2.329 keV (illustrated in Fig. 1, left). The decay of the isomer is dominated by $E2$ transition ($M1$ is forbidden). The isomer has a relatively long half-life $T_{1/2}$ around 15 min for the bare nucleus. (The nonradiative half-life via internal conversion is 24.2 μs [44]. For highly charged ions or the bare nucleus, internal-conversion channels are closed, and only the radiative half-life is of concern.) The nuclear reduced matrix element $\langle I_g||\mathcal{M}_L^\tau||I_e\rangle$ can be determined from the reduced nuclear transition probability $B(\tau L, I_e \to I_g) = [L]/(4\pi[I_e])|\langle I_g||M_L^\tau||I_e\rangle|^2$. In the current work, the value for $B(E2, I_e \to I_g)$ is adopted as 0.127 W.u. [44].

The B-like ^{205}Pb ion has an unpaired $2p_{1/2}$ electron in the ground configuration ($1s^2 2s^2 2p\ {}^2P_{1/2}$). Without considering hyperfine mixing, this $2p_{1/2}$ electron leads to a hyperfine structure as shown in Fig. 1 (middle). The isomeric state splits into two levels with $F_e = 1$ (energy shift 0.017 eV) and $F_e = 0$ (energy shift −0.051 eV). The ground state splits into two levels with $F_g = 3$ (energy shift 0.019 eV) and $F_g = 2$ (energy shift −0.027 eV). Three $E2$ transitions are possible from the upper two levels to the lower two levels, as listed in Table I (left part, without NHM). In the calculation, we have taken the magnetic moments of the nuclear ground and isomeric states to be $0.71\mu_N$ [44] and $0.64\mu_N$ [46], respectively. The magnetic moment of the isomeric state is calculated using the Schmidt model.

The inclusion of NHM leads to dramatic changes to the nuclear transitions, as listed in Table I (right part, with NHM). [NHM causes negligible additional energy-level shifts though, as illustrated in Fig. 1 (right).] The most notable change is the opening of a new $M1$ transition channel from the $F_e = 1$ level to the $F_g = 2$ level that is otherwise forbidden. This new $M1$ channel has a much higher transition rate than the $E2$ counterpart, reducing the lifetime of the $F_e = 1$ level by over 4 orders of magnitude, from 15 min to 32 ms. One also notices that the $E2$ transition channels from $F_e = 1$ to $F_g = 2$ and to $F_g = 3$ have also been accelerated due to NHM. The $E2$ transition channel from $F_e = 0$ to $F_g = 2$ remains unchanged, because the mixing coefficient is zero.

The $2p_{1/2}$ electronic ground state does not contribute to the mixing coefficient due to the angular-momentum selection rules. The $2p_{3/2}$ electronic excited state (denoted $\tilde{\varepsilon}$) is 2.356 keV above the $2p_{1/2}$ state. One immediately notices that this electronic transition energy is close to the nuclear transition energy of 2.329 keV, allowing an efficient mixing between $|F_e m_{F_e}(I_e \gamma_\varepsilon J_\varepsilon)\rangle$ (i.e., nucleus in excited state e and electron in ground state ε) and $|F_e m_{F_e}(I_g \gamma_{\tilde{\varepsilon}} J_{\tilde{\varepsilon}})\rangle$ (i.e., nucleus in ground state g and electron in excited state $\tilde{\varepsilon}$).

TABLE I. Nuclear transitions in the $^{205}Pb^{77+}$ ion (left part) without NHM and (right part) with NHM. Note the new $M1$ transition channel that is opened by the NHM effect.

Without NHM				With NHM			
Transition	Type	Rate (s^{-1})	$T_{1/2}$	Transition	Type	Rate (s^{-1})	$T_{1/2}$
$\|F_e=1\rangle \to \|F_g=2\rangle$	$E2$	1.7×10^{-4}	68 min	$\|F_e=1\rangle_+ \to \|F_g=2\rangle_+$	$E2$	1.7×10^{-2}	41 s
					$M1$	2.2×10^{1}	32 ms
$\|F_e=1\rangle \to \|F_g=3\rangle$	$E2$	6.2×10^{-4}	19 min	$\|F_e=1\rangle_+ \to \|F_g=3\rangle_+$	$E2$	2.6×10^{-1}	2.7 s
$\|F_e=0\rangle \to \|F_g=2\rangle$	$E2$	7.9×10^{-4}	15 min	$\|F_e=0\rangle_+ \to \|F_g=2\rangle_+$	$E2$	7.9×10^{-4}	15 min

In fact, the newly opened $M1$ transition is mainly between the mixed component of $|F_e m_{F_e}(I_g \gamma_{\tilde{\varepsilon}} J_{\tilde{\varepsilon}})\rangle$ state and the $|F_g m_{F_g}(I_g \gamma_\varepsilon J_\varepsilon)\rangle$ state. Higher electronic states are far off resonance. As a result, there is a single dominant mixing coefficient $c_{e\varepsilon,g\tilde{\varepsilon}}$ involving the electronic $2p_{3/2}$ state, and other mixing coefficients are negligible in comparison.

We use the GRASP2K package [47] to calculate the energy levels of the B-like ^{205}Pb ion. This package is based on a fully relativistic multiconfiguration Dirac-Hartree-Fock method. An active-set approach has been employed to systematically enhance the precision of the atomic calculation. Our calculation of the energy of the $2p_{3/2}$ state agrees very closely to the result given in Ref. [48]. With the relativistic wave functions numerically solved using the GRASP2K package, the dominant mixing coefficient $c_{e\varepsilon,g\tilde{\varepsilon}}$ is calculated to be

$$c_{e\varepsilon,g\tilde{\varepsilon}} = -1.97 \times 10^{-5}$$

for $F_e = 1$. It is zero for $F_e = 0$ due to selection rules. Then, the nuclear transition rates between the isomeric and the ground states can be calculated using Eqs. (8)–(10). This is how the results in Table I are obtained.

Further discussions.—Up till now, the NHM effect has not been observed experimentally, and proposals of experimental verification have been solely based on ^{229}Th ions [30–36]. ^{205}Pb offers an alternative target for the experimental validation. Besides, the decay signal is 2.329-keV photons in the x-ray range which can be detected with very high efficiency.

The half-life of the ^{205}Pb nucleus is very long (1.73×10^7 yr [44]) to allow for long-time storage and experimentation. A potential experiment to verify the NHM effect can be performed using intense-laser optical excitation in storage rings [49–51], in which the ions are accelerated to move with relativistic velocities. With the relativistic Doppler effect, the laser peak intensity I_r, angular frequency ω_r, and duration t_r in the ion rest frame are related to the corresponding values in the laboratory frame (I_b, ω_b, t_b) by $I_r = (2\gamma)^2 I_b$, $\omega_r = 2\gamma\omega_b$, and $t_r = t_b/2\gamma$ [52,53], with γ being the Lorentz factor.

Consider using a 267-nm ($\omega_b = 4.65$ eV, third harmonic of 800 nm) intense laser pulse to resonantly excite the ^{205}Pb nucleus. The Lorentz factor required is about $\gamma = 250$, which can be achieved at the Large Hadron Collider (LHC) at CERN (the maximal achievable Lorentz factor is about 3000 [54]). Assume the laser pulse has a peak intensity $I_b = 10^{13}$ W/cm^2, duration $t_b = 1$ ns, and a Gaussian beam profile with waist 16 μm (which is the radius of the ion bunch at the LHC [54]). The energy of the laser pulse is then about 80 mJ. The intensity I_r and the duration t_r in the ion rest frame are 2.5×10^{18} W/cm^2 and 2 ps, respectively. With the NHM effect, the nuclear excitation probability by this laser pulse is calculated to be 7.4×10^{-5}. (Detailed formulas of calculating optical excitation can be found in [27].) The depletion of the electronic ground state is calculated to be negligible, because the transition energy between the electronic ground and excited states are far off resonance with the optical frequency ω_r. Every bunch contains about 10^8 target ions at the LHC [54], so the number of excited nuclei is about 7.4×10^3 per pulse per bunch. These excited nuclei are expected to emit a similar number of 2.329-keV x-ray photons within the second following optical excitation, and these photons can be detected and analyzed.

Alternatively, the experiment may be performed using a combination of electron beam ion traps [55,56] and x-ray free electron lasers (XFELs), as seen in previous studies [57]. Let us consider the European XFEL, which can produce 2.329-keV 100-fs x-ray pulses in bunches [58]. Each bunch, lasting 0.6 ms and comprising 2700 pulses, is followed by a 100-ms gap before the next bunch. Given the isomeric state's half-life of 32 ms, considerably longer than the bunch duration but shorter than the gap time, this bunch-gap cycle naturally facilitates excitation and detection, repeating 10 times per second. With approximately 10^{13} photons per pulse and an intensity exceeding 10^{18} W/cm^2 [58], the nuclear excitation probability for a single nucleus by one bunch is calculated to be approximately 10^{-3}. Assuming a number of 100 ions irradiated by the x-ray pulses, the excitation efficiency is approximately one nucleus per ten bunches. Consequently, one decaying photon datum would be anticipated every second (i.e., every ten gaps), with its decay time registered (time zero is set at the end of each bunch). Detecting such decaying photons would directly confirm the NHM effect, as the excitation efficiency would be negligibly small without this effect. With sufficient decaying-photon data collected over experimental time along with decay-time information, the isomeric state's half-life could also be determined. Moreover, future XFEL facilities like Linac Coherent Light Source II (LCLS-II) [59] or Shanghai High Repetition Rate XFEL and Extreme Light Facility (SHINE) [60], designed to output 1 million pulses per second, hold promise for enhancing data collection efficiency.

Lastly, the bound internal conversion (BIC) process [61] is worth mentioning. In this process, the excited nucleus undergoes nonradiative decay by exciting an electron, provided the energy mismatch between the transitions is compensated by their respective widths, particularly the width of the electronic excited state. However, in the ^{205}Pb ion, the natural width of the $2p_{3/2}$ state is only 1.4×10^{-4} eV, significantly smaller than the 27-eV mismatch. Consequently, the excited nucleus decays radiatively without interference from BIC.

Conclusion.—In this Letter, we have uncovered a novel nuclear system, extending beyond the scope of ^{229}Th, showcasing significant NHM effects. Our investigation

into B-like ^{205}Pb ions reveals an extraordinary 4-orders-of-magnitude decrease in the half-life of the nuclear isomeric state—from 15 min to a mere 32 ms. Remarkably, the ^{205}Pb nucleus features a transition energy of 2.329 keV, and non-negligible NHM effect would not be expected from current understanding of the community. The unexpected substantial NHM effect in B-like ^{205}Pb ions is attributed to a previously unexplored mechanism: the opening of a forbidden $M1$ channel by NHM. Notably, electronic excited states are found to participate in the NHM process for the first time. Our study represents a significant stride forward in comprehending the NHM effect and opens up alternative avenues for experimental verification and investigation. This new understanding holds the potential for actively and efficiently controlling atomic nuclei, particularly through advanced light sources like intense lasers, synchrotron radiations, and x-ray free electron lasers.

The authors acknowledge helpful discussions with Mr. Hanxu Zhang. This work was supported by National Safety Academic Fund Grant No. U2330401 and National Natural Science Foundation of China Grant No. 12088101.

*xwang@gscaep.ac.cn

[1] G. D. Dracoulis, P. M. Walker, and F. G. Kondev, Rep. Prog. Phys. **79**, 076301 (2016).
[2] H. Grawe, K. Langanke, and G. Martínez-Pinedo, Rep. Prog. Phys. **70**, 1525 (2007).
[3] G. W. Misch, S. K. Ghorui, P. Banerjee, Y. Sun, and M. R. Mumpower, Astrophys. J. Suppl. Ser. **252**, 2 (2020).
[4] E. Peik and C. Tamm, Europhys. Lett. **61**, 181 (2003).
[5] W. G. Rellergert, D. DeMille, R. R. Greco, M. P. Hehlen, J. R. Torgerson, and E. R. Hudson, Phys. Rev. Lett. **104**, 200802 (2010).
[6] C. J. Campbell, A. G. Radnaev, A. Kuzmich, V. A. Dzuba, V. V. Flambaum, and A. Derevianko, Phys. Rev. Lett. **108**, 120802 (2012).
[7] E. Peik, T. Schumm, M. S. Safronova, A. Pálffy, J. Weitenberg, and P. G. Thirolf, Quantum Sci. Technol. **6**, 034002 (2021).
[8] P. Walker and G. Dracoulis, Nature (London) **399**, 35 (1999).
[9] J. J. Carroll, S. A. Karamian, L. A. Rivlin, and A. A. Zadernovsky, Hyperfine Interact. **135**, 3 (2001).
[10] A. A. Zadernovsky and J. J. Carroll, Hyperfine Interact. **143**, 153 (2002).
[11] L. Rivlin and A. Zadernovsky, Laser Phys. **20**, 971 (2010).
[12] E. V. Tkalya, Phys. Rev. Lett. **106**, 162501 (2011).
[13] L. Marmugi, P. M. Walker, and F. Renzoni, Phys. Lett. B **777**, 281 (2018).
[14] M. Morita, Prog. Theor. Phys. **49**, 1574 (1973).
[15] V. I. Goldanskii and V. A. Namiot, Phys. Lett. **62B**, 393 (1976).
[16] E. V. Tkalya, Nucl. Phys. **A539**, 209 (1992).
[17] S. Kishimoto, Y. Yoda, M. Seto, Y. Kobayashi, S. Kitao, R. Haruki, T. Kawauchi, K. Fukutani, and T. Okano, Phys. Rev. Lett. **85**, 1831 (2000).
[18] H. Zhang and X. Wang, Front. Phys. **11**, 1166566 (2023).
[19] R. Röhlsberger, K. Schlage, B. Sahoo, S. Couet, and R. Rüffer, Science **328**, 1248 (2010).
[20] R. Röhlsberger, H.-C. Wille, K. Schlage, and B. Sahoo, Nature (London) **482**, 199 (2012).
[21] T. Masuda *et al.*, Nature (London) **573**, 238 (2019).
[22] A. Zilges, D. L. Balabanski, J. Isaak, and N. Pietralla, Prog. Part. Nucl. Phys. **122**, 103903 (2022).
[23] W. Wang, J. Zhou, B. Liu, and X. Wang, Phys. Rev. Lett. **127**, 052501 (2021).
[24] W. Wang, H. Zhang, and X. Wang, J. Phys. B **54**, 244001 (2021).
[25] X. Wang, Phys. Rev. C **106**, 024606 (2022).
[26] J. Qi, H. Zhang, and X. Wang, Phys. Rev. Lett. **130**, 112501 (2023).
[27] W. Wang and X. Wang, Phys. Rev. Res. **5**, 043232 (2023).
[28] V. L. Lyuboshitz, V. A. Onishchuk, and M. I. Podgoretskij, Sov. J. Nucl. Phys. **3**, 420 (1966), https://www.osti.gov/biblio/4533457.
[29] J. Szerypo, R. Barden, Ł. Kalinowski, R. Kirchner, O. Klepper, A. Płochocki, E. Roeckl, K. Rykaczewski, D. Schardt, and J. Żylicz, Nucl. Phys. **A507**, 357 (1990).
[30] S. Wycech and J. Żylicz, Acta Phys. Pol. B **24**, 637 (1993), https://www.actaphys.uj.edu.pl/R/24/3/637/pdf.
[31] F. F. Karpeshin, S. Wycech, I. M. Band, M. B. Trzhaskovskaya, M. Pfützner, and J. Żylicz, Phys. Rev. C **57**, 3085 (1998).
[32] K. Pachucki, S. Wycech, J. Żylicz, and M. Pfützner, Phys. Rev. C **64**, 064301 (2001).
[33] K. Beloy, Phys. Rev. Lett. **112**, 062503 (2014).
[34] E. V. Tkalya and A. V. Nikolaev, Phys. Rev. C **94**, 014323 (2016).
[35] V. M. Shabaev, D. A. Glazov, A. M. Ryzhkov, C. Brandau, G. Plunien, W. Quint, A. M. Volchkova, and D. V. Zinenko, Phys. Rev. Lett. **128**, 043001 (2022).
[36] J. Jin, H. Bekker, T. Kirschbaum, Y. A. Litvinov, A. Pálffy, J. Sommerfeldt, A. Surzhykov, P. G. Thirolf, and D. Budker, Phys. Rev. Res. **5**, 023134 (2023).
[37] J. Jeet, C. Schneider, S. T. Sullivan, W. G. Rellergert, S. Mirzadeh, A. Cassanho, H. P. Jenssen, E. V. Tkalya, and E. R. Hudson, Phys. Rev. Lett. **114**, 253001 (2015).
[38] A. Yamaguchi, M. Kolbe, H. Kaser, T. Reichel, A. Gottwald, and E. Peik, New J. Phys. **17**, 053053 (2015).
[39] E. Peik and M. Okhapkin, C.R. Phys. **16**, 516 (2015).
[40] S. Stellmer, G. Kazakov, M. Schreitl, H. Kaser, M. Kolbe, and T. Schumm, Phys. Rev. A **97**, 062506 (2018).
[41] S. G. Nielsen, M. Rehkämper, and A. N. Halliday, Geochim. Cosmochim. Acta **70**, 2643 (2006).
[42] R. G. A. Baker, M. Schönbächler, M. Rehkämper, H. M. Williams, and A. N. Halliday, Earth Planet. Sci. Lett. **291**, 39 (2010).
[43] A. P. Tonchev *et al.*, EPJ Web Conf. **178**, 04003 (2018).
[44] Nuclear Structure and Decay Databases (2023), https://www.nndc.bnl.gov/.
[45] C. Schwartz, Phys. Rev. **97**, 380 (1955).
[46] T. Schmidt, Z. Phys. A **106**, 358 (1937).

[47] P. Jönsson, G. Gaigalas, J. Bieron, C. F. Fischer, and I. P. Grant, Comput. Phys. Commun. **184**, 2197 (2013).
[48] A. N. Artemyev, V. M. Shabaev, I. I. Tupitsyn, G. Plunien, A. Surzhykov, and S. Fritzsche, Phys. Rev. A **88**, 032518 (2013).
[49] J. W. Xia *et al.*, Nucl. Instrum. Methods Phys. Res., Sect. A **488**, 11 (2002).
[50] B. Franzke, H. Geissel, and G. Münzenberg, Spectrom. Rev. **27**, 428 (2008).
[51] W. Nörtershäuser and R. Sánchez, Phys. Scr. T **166**, 014020 (2015).
[52] T. J. Bürvenich, J. Evers, and C. H. Keitel, Phys. Rev. Lett. **96**, 142501 (2006).
[53] T. Kirschbaum, N. Minkov, and A. Pálffy, Phys. Rev. C **105**, 064313 (2022).
[54] D. Budker J. R. C. López-Urrutia, A. Derevianko, V. V. Flambaum, M. W. Krasny, A. Petrenko, S. Pustelny, A. Surzhykov, V. A. Yerokhin, and M. Zolotorev, Ann. Phys. (Berlin) **532**, 2000204 (2020).
[55] M. A. Levine, R. E. Marrs, J. R. Henderson, D. A. Knapp, and M. B. Schneider, Phys. Scr. **1988**, 157 (1988).
[56] A. Lapierre, J. R. CrespoLopez-Urrutia, J. Braun, G. Brenner, H. Bruhns *et al.*, Phys. Rev. A **73**, 052507 (2006).
[57] S. Bernitt *et al.*, Nature (London) **492**, 225 (2012).
[58] M. Izquierdo, Technical design report XFEL.EU TR-2022-001A (2022).
[59] J. N. Galayda, The LCLS-II: A high power upgrade to the LCLS. https://www.osti.gov/servlets/purl/1604347 (2018).
[60] T. Liu *et al.*, Front. Phys. **11**, 1172368 (2023).
[61] F. F. Karpeshin, M. R. Harston, F. Attallah, J. F. Chemin, J. N. Scheurer, I. M. Band, and M. B. Trzhaskovskaya, Phys. Rev. C **53**, 1640 (1996).